**International Journal of Environmental Sciences**
ISSN: 2229-7359
Vol. 11 No. 22s, 2025
https://www.theaspd.com/ijes.php

# Development Of Lipid-Based Nanoscale Delivery Platforms Incorporating Enicostemma Littorale Extract For Targeted Glycemic Modulation

**Farhad F Mehta[1], L.Rajesh Patro [2], Gunosindhu Chakraborthy [3], Dillip Kumar Brahma[4], Vijay Sharma [5], B. Sree Giri Prasad [6], Nusrat Sheikh [7], Mohankumar S. Raut [8]***

[1]Assistant Professor, School of Pharmaceutical Sciences, U.T.D, R.G.P.V University, Bhopal, Madhya Pradesh 462033.

[2]Principal & Professor, UMU School of Pharmacy, Usha Martin University, Angara, Ranchi, Jharkhand 835103

[3]Professor and Principal, Parul Institute of Pharmacy and Research, Parul University, Waghodia, Dist. Vadodara, Gujarat 391760

[4]Principal & Professor, Department of Pharmacy, Netaji Subhash University, Jamshedpur, Jharkhand 831012

[5]Professor, Faculty of Pharmacy, IFTM University, Moradabad, UP 244102

[6]Professor, Nalla Narasimha Reddy Educational Society's Group of Institutions, Medchal - Malkajgiri, Ghatkesar, Hyderabad, Telangana 500088.

[7]Assistant professor, Chandigarh Group of Colleges Jhanjeri, Mohali, Punjab, India 140307, Chandigarh School of Business, Department of Forensic Sciences.

[8]Professor, Department of Balroga, Datta Meghe Ayurvedic Medical College Hospital and Research Centre, Nagpur, Maharashtra 441110

***Abstract***

*Diabetes mellitus continues to be a major global health burden due to its rising prevalence and the limitations of conventional therapies, which often suffer from poor bioavailability, instability, and systemic side effects. Phytomedicine has been increasingly explored as an alternative approach, with Enicostemma littorale (EL) recognized for its potent antihyperglycemic, antioxidant, and insulin-sensitizing activities. However, the therapeutic potential of EL is restricted by its poor solubility and rapid metabolism. In the present study, lipid-based nanoscale delivery systems incorporating EL extract were developed to enhance its solubility, stability, and bioavailability for improved glycemic modulation. Nanoparticles were prepared by high-pressure homogenization using glyceryl monostearate, Compritol, Precirol, and stearic acid as lipid matrices, stabilized with Poloxamer 188, Tween 80, and lecithin. Compatibility of the extract with excipients was confirmed by FTIR, DSC. The optimized formulation exhibited a mean particle size of 162.4 ± 4.8 nm, PDI of 0.214, and zeta potential of –28.6 mV, indicating good stability. SEM analysis revealed spherical morphology with uniform distribution. The entrapment efficiency was 84.7 ± 2.3% with a production yield of 88.5 ± 3.2%. In vitro release studies demonstrated a biphasic release with ~22% drug release in the first 2 h followed by sustained release up to 78.6% at 24 h. Release was pH-dependent, showing better stability and controlled release under intestinal (74%) and physiological (79%) conditions compared to gastric pH (38%). Kinetic modeling indicated that the Higuchi model ($R^2$ = 0.981) provided the best fit, confirming diffusion-controlled release, while the Korsmeyer–Peppas model (n = 0.64) suggested anomalous transport. Overall, the study confirmed that lipid-based nanoscale carriers significantly enhanced encapsulation, stability, and controlled release of EL extract, highlighting their potential as an effective oral therapeutic strategy for targeted glycemic modulation in diabetes management.*

***Keywords:*** Enicostemma littorale; *lipid-based nanoparticles; solid lipid nanoparticles; phytomedicine; diabetes mellitus; glycemic modulation; nanocarrier system.*

## INTRODUCTION

Diabetes mellitus is one of the most prevalent metabolic disorders worldwide and continues to pose a significant health and economic burden across both developed and developing nations [1],[2]. The global prevalence of diabetes has been steadily increasing due to sedentary lifestyles, poor dietary habits, and genetic

predispositions, with projections indicating a substantial rise in the number of cases in the coming decades [3],[4]. Despite the availability of multiple therapeutic agents and treatment strategies, effective long-term management remains a challenge. Conventional therapies, although widely used, are often limited by poor oral bioavailability, short half-life, systemic side effects, and issues of poor patient compliance, all of which compromise therapeutic success [5],[6]. In this context, phytomedicine has emerged as an important complementary approach to glycemic management [7],[8]. Among several medicinal plants, *Enicostemma littorale* (EL), commonly known as "Mamejava," has attracted considerable attention due to its rich phytoconstituents such as swertiamarin, flavonoids, and xanthones, which are reported to exert potent antihyperglycemic, antioxidant, and insulin-sensitizing effects [9]–[11]. However, the therapeutic promise of EL is hindered by limitations including poor solubility, rapid metabolism, and instability of its bioactive compounds, restricting its clinical applicability in diabetes management [12]. Nanotechnology-based delivery systems offer a promising solution to these challenges. Lipid-based nanosystems such as solid lipid nanoparticles (SLNs), nanostructured lipid carriers (NLCs), liposomes, and nanoemulsions have shown great potential in improving solubility, enhancing stability, prolonging circulation time, and enabling targeted delivery of bioactives [13]. These carriers not only protect plant-derived compounds from premature degradation but also allow controlled release and site-specific drug delivery, thereby improving therapeutic efficacy and minimizing side effects [14]. Considering these advantages, the rationale of the present investigation lies in the development of a stable, bioavailable, and targeted nanoscale lipidic delivery platform for EL extract to optimize its antidiabetic potential. To date, no systematic study has been reported on formulating lipid-based nanocarriers specifically for *Enicostemma littorale*, which highlights a significant research gap in the field of herbal nanomedicine. Therefore, the objective of this study is to design, develop, and evaluate lipid-based nanoscale delivery systems incorporating *Enicostemma littorale* extract, with the aim of enhancing its bioavailability and therapeutic efficacy in targeted glycemic modulation. This approach not only addresses the shortcomings of conventional delivery but also provides a novel pathway for integrating phytomedicine with advanced nanotechnology for effective diabetes management.

## MATERIALS AND METHODS

### Plant Material Collection and Authentication

The aerial parts of *Enicostemma littorale* were collected during the flowering season (July–August) from the herbal-rich regions of Anand district, Gujarat, India, where the plant grows abundantly in semi-arid soil conditions. The plant specimen was identified and authenticated at Department of Botany, Faculty of Science, The Maharaja Sayajirao University of Baroda, Vadodara, Gujarat, India. A voucher specimen (Voucher No. EL/PHAR/2025/01) was prepared and deposited in the departmental herbarium of The Maharaja Sayajirao University of Baroda for future reference and record maintenance.

### Processing of Plant Material

The collected plant material was cleaned with distilled water to remove dirt and impurities. The samples were shade dried at room temperature (25–28 °C) for 10–12 days and then powdered using a mechanical grinder. The coarse powder was sieved through a #40 mesh to ensure uniform particle size before extraction.

### Extraction Procedure

A total of 500 g of powdered *E. littorale* was subjected to hydroalcoholic maceration using ethanol:water (70:30 v/v) as the extraction solvent. The plant material was soaked in the solvent in a ratio of 1:10 (w/v) for 72 hours with occasional stirring. The extract was filtered through Whatman No. 1 filter paper, and the marc was re-extracted twice to ensure maximum yield. The combined extracts were concentrated under reduced pressure using a rotary vacuum evaporator (Buchi, Switzerland) at 40–45 °C to obtain a thick semisolid mass. The dried extract was stored in amber-colored airtight containers at 4 °C. The extraction yield (%) was calculated based on the dried weight of the extract obtained [15].

### Formulation of Lipid-Based Nanocarriers

### Selection of Lipids and Excipients

For the formulation of lipid-based nanocarriers, both solid and stabilizing agents were selected based on their safety profile, compatibility with plant extract, and reported use in nanocarrier formulations. Glyceryl

monostearate (GMS), stearic acid, Compritol® 888 ATO, and Precirol® ATO 5 were evaluated as lipid matrices due to their Generally Recognized as Safe (GRAS) status and ability to entrap lipophilic phytoconstituents. Poloxamer 188, Tween 80, and lecithin were chosen as surfactant and co-surfactant systems to enhance emulsification, provide colloidal stability, and reduce particle aggregation during storage [16].

**Preparation by High-Pressure Homogenization**

The hot homogenization technique was employed as the primary method for preparing *Enicostemma littorale* extract-loaded lipid nanocarriers:

1. **Lipid Phase Preparation:** The weighed quantity of lipid (GMS, stearic acid, Compritol, or Precirol) was melted at 70–75 °C, maintained above the lipid's melting point. The *E. littorale* hydroalcoholic extract (pre-dissolved in a small volume of ethanol) was incorporated into the molten lipid under magnetic stirring to ensure uniform dispersion.
2. **Aqueous Phase Preparation:** A hot aqueous solution of surfactant/co-surfactant (Poloxamer 188, Tween 80, and lecithin, alone or in combination) was prepared separately at the same temperature to avoid premature solidification.
3. **Pre-emulsion Formation:** The lipid phase was added dropwise to the aqueous surfactant solution under continuous stirring at 10,000 rpm using a high-speed homogenizer (Ultra-Turrax T25, IKA, Germany) for 5–10 minutes to form a coarse pre-emulsion.
4. **High-Pressure Homogenization:** The pre-emulsion was then subjected to high-pressure homogenization (EmulsiFlex-C3, Avestin, Canada) at 800–1000 bar for 3–5 cycles to reduce the particle size and achieve uniform nanoscale dispersion.
5. **Cooling and Solidification:** The hot nanoemulsion was rapidly cooled to room temperature under continuous stirring, leading to solidification of the lipid phase and formation of solid lipid nanoparticles (SLNs) or nanostructured lipid carriers (NLCs), depending on the lipid composition used [17].

**Ultrasonication for Size Reduction**

To further reduce the particle size and improve homogeneity, the coarse dispersions obtained from either hot homogenization or solvent evaporation method were probe-sonicated for 5–10 minutes in pulse mode (30 s on, 10 s off) while maintaining the temperature in an ice bath to avoid thermal degradation of phytoconstituents.

**Optimization Strategy**

A series of formulations were prepared by varying lipid type (GMS, stearic acid, Compritol, Precirol) and surfactant concentration (Poloxamer 188, Tween 80, lecithin). The optimized formulation was selected based on particle size (<200 nm), polydispersity index (PDI < 0.3), high entrapment efficiency (>80%), and stable zeta potential (> ±25 mV) [18].

**Preformulation Studies**

**Fourier Transform Infrared Spectroscopy (FTIR) for Compatibility**

FTIR spectroscopy was performed to evaluate possible chemical interactions between *Enicostemma littorale* extract and selected excipients. Samples of pure extract, individual lipids (GMS, stearic acid, Compritol, Precirol), surfactants (Poloxamer 188, Tween 80, lecithin), and physical mixtures (extract + excipients in 1:1 ratio) were analyzed. Each sample was triturated with dry potassium bromide (KBr) and compressed into pellets under a hydraulic press. The spectra were recorded using an FTIR spectrophotometer (Bruker Tensor 27, Germany) in the range of 4000–400 $cm^{-1}$ at a resolution of 4 $cm^{-1}$. The characteristic peaks of major functional groups of swertiamarin and related phytoconstituents were compared with the spectra of physical mixtures to check for any shift, disappearance, or formation of new peaks, which would indicate drug–excipient incompatibility [19].

**Differential Scanning Calorimetry (DSC) for Thermal Analysis**

Differential scanning calorimetry was employed to assess the thermal behavior of *E. littorale* extract and its compatibility with lipids and surfactants. Approximately 5–10 mg of each sample (pure extract, excipients, and physical mixtures) was placed in a sealed aluminum pan and analyzed using a DSC instrument (Mettler Toledo DSC 822e, Switzerland). The samples were heated from 30 °C to 300 °C at a scanning rate of 10

°C/min under a nitrogen atmosphere (flow rate 40 mL/min). Thermograms were obtained for each sample, and melting point, onset temperature, and enthalpy changes were recorded. Absence of significant peak shifts or changes in enthalpy values in physical mixtures confirmed the compatibility of extract with excipients [20].

**Characterization of Nanoparticles**

**Particle Size and Polydispersity Index (PDI)**

The mean particle size, size distribution, and polydispersity index (PDI) of *E. littorale* extract-loaded nanoparticles were determined by Dynamic Light Scattering (DLS) using a Zetasizer Nano ZS (Malvern Instruments, UK). The nanoparticle dispersion was diluted (1:100 v/v) with double-distilled water to avoid multiple scattering effects before analysis. Measurements were carried out at 25 °C, and results were reported as mean hydrodynamic diameter (Z-average) and PDI. A PDI value below 0.3 was considered indicative of a narrow and uniform size distribution [21].

**Zeta Potential**

The surface charge of nanoparticles was measured by laser Doppler electrophoresis using the same instrument (Malvern Zetasizer Nano ZS). Samples were appropriately diluted with 1 mM KCl solution and placed in a disposable folded capillary cell. Measurements were recorded at 25 °C. Zeta potential values beyond ±25 mV were considered indicative of good electrostatic stability.

**Morphology (SEM)**

The surface morphology and shape of the prepared nanoparticles were evaluated using advanced imaging techniques such as Scanning Electron Microscopy (SEM), a drop of the nanoparticle dispersion was carefully placed onto an aluminum stub and allowed to air dry to ensure proper adhesion. The dried sample was then sputter-coated with a thin layer of gold (~10 nm) under vacuum to make the surface conductive and prevent charging during imaging. The coated sample was observed using a JEOL JSM-7600F (Japan) scanning electron microscope operated at an accelerating voltage of 10 kV. This provided detailed micrographs of the particle surface, allowing assessment of shape, surface smoothness, and uniformity. TEM and AFM analyses were further employed to complement SEM findings, offering nanoscale visualization of the internal structure, topology, and three-dimensional surface profile of the nanoparticles, thereby confirming their spherical shape, smooth morphology, and nanoscale dimensions [22].

**Entrapment Efficiency and Drug Loading**

Entrapment efficiency (EE%) and drug loading (DL%) of the prepared lipid-based nanoparticles were determined using the ultracentrifugation method. A measured volume of the nanoparticle dispersion was subjected to ultracentrifugation at 30,000 rpm for 30 minutes at 4 °C using a Beckman Coulter Optima XPN-100 (USA). After centrifugation, the supernatant containing the free drug (unentrapped fraction of *Enicostemma littorale* extract) was carefully collected and analyzed spectrophotometrically at 235 nm using swertiamarin as the reference marker on a UV–Vis spectrophotometer (Shimadzu UV-1800, Japan). The amount of drug present in the supernatant was subtracted from the total amount of drug initially added to the formulation to determine the entrapped portion. Entrapment efficiency was then calculated as the percentage of the drug encapsulated within the nanoparticles relative to the total drug used, while drug loading was calculated as the proportion of the entrapped drug with respect to the total weight of nanoparticles obtained [23].

The calculations were carried out using the following equations:

$$Entrapment\ Efficiency\ (EE\%) = \frac{(Total\ drug - Free\ drug)}{Total\ drug} \times 100$$

$$Drug\ Loading\ (DL\%) = \frac{Entrapped\ drug}{Total\ weight\ of\ nanoparticles} x100$$

**Percentage Yield**

The percentage yield of the prepared nanoparticles was determined by comparing the total weight of lyophilized nanoparticles obtained with the initial total weight of drug and excipients used in the formulation. This calculation provided an indication of the efficiency of the formulation process in terms of material recovery. The yield was calculated using the following equation:

$$\%\,Yield = \frac{Weight\ of\ nanoparticles\ recovered}{Total\ weight\ of\ drug + excipients\ used} \text{x}100$$

For this purpose, the freshly prepared nanoparticle dispersions were subjected to freeze-drying (lyophilization) in order to obtain a dry, free-flowing powder. Mannitol (5% w/v) was employed as a cryoprotectant to prevent aggregation of nanoparticles during the freezing and drying process. Lyophilization was carried out using a Labconco FreeZone 2.5 Plus freeze-dryer (USA) at –50 °C and 0.04 mbar chamber pressure until complete sublimation of water was achieved. The dried nanoparticles were collected, weighed, and stored in airtight amber vials at 4 °C until further use. This process ensured long-term stability and accurate determination of formulation yield [24].

**In Vitro Drug Release Studies**

The in vitro release profile of *Enicostemma littorale* extract from the lipid-based nanoparticles was investigated using the dialysis bag diffusion method. A dispersion of nanoparticles equivalent to 10 mg of the extract was accurately measured and loaded into a pre-activated dialysis membrane (molecular weight cut-off: 12–14 kDa). The sealed bag was then immersed in 50 mL of release medium maintained at 37 ± 0.5 °C under continuous stirring at 100 rpm using a USP dissolution apparatus II (paddle method). This setup ensured uniform mixing and minimized diffusional boundary effects. Release studies were conducted under three simulated physiological conditions to mimic different stages of drug transit: (i) pH 1.2 (0.1 N HCl) to represent gastric fluid, (ii) pH 6.8 phosphate buffer to represent intestinal fluid, and (iii) pH 7.4 phosphate buffer to represent systemic plasma conditions. At predetermined intervals (0.5, 1, 2, 4, 6, 8, 12, and 24 hours), 2 mL aliquots were withdrawn from the dissolution medium and immediately replaced with an equal volume of fresh medium maintained at the same temperature to preserve sink conditions throughout the experiment. The collected samples were filtered through 0.45 μm syringe filters to remove any residual particulate matter, and the drug concentration was quantified spectrophotometrically at 235 nm using swertiamarin as the marker compound. The cumulative percentage of drug release was calculated at each time point, and release profiles were plotted to compare the behavior of nanoparticles in different pH environments [25].

**Drug Release Kinetics**

The cumulative in vitro drug release data of *Enicostemma littorale* extract-loaded lipid nanoparticles were analyzed to elucidate the release mechanism. The release profiles were fitted to various kinetic models, including the zero-order model (cumulative percentage drug release versus time), first-order model (log percentage drug remaining versus time), Higuchi model (cumulative percentage drug release versus square root of time), and the Korsmeyer–Peppas model (log cumulative drug release versus log time). The regression coefficient ($R^2$) values for each model were calculated to determine the best-fit kinetic model. Additionally, the release exponent (n) derived from the Korsmeyer–Peppas equation was used to characterize the drug release mechanism, where $n \leq 0.5$ indicated Fickian diffusion, $0.5 < n < 1$ suggested anomalous (non-Fickian) transport, and $n = 1$ indicated case-II transport (zero-order release controlled by polymer relaxation or erosion) [26].

## RESULTS AND DISCUSSION

### Preformulation Results

**FTIR Compatibility**

The *Enicostemma littorale* (EL) extract showed a broad O–H stretch (polyphenols/iridoid glycosides) at ~3368 $cm^{-1}$, C–H stretches at 2922/2852 $cm^{-1}$, a carbonyl band at 1708–1716 $cm^{-1}$ (lactone/ester), aromatic/olefinic C=C at 1621 $cm^{-1}$, and strong C–O–C/C–O bands at 1158–1034 $cm^{-1}$. Lipids exhibited the expected ester C=O at 1736–1743 $cm^{-1}$ with intense $CH_2$ bands at ~2918/2849 $cm^{-1}$; lecithin showed P=O at ~1236 $cm^{-1}$ and P–O–C near 1064 $cm^{-1}$; Poloxamer had a prominent ether band near 1105 $cm^{-1}$; Tween-80 displayed a strong 1738 $cm^{-1}$ C=O. In 1:1 physical mixture (EL:excipient), all diagnostic peaks of both extract and excipients were retained with only trivial shifts (≤3–5 $cm^{-1}$) and no new bands or band disappearance, indicating no chemical interaction and good FTIR compatibility.

**International Journal of Environmental Sciences**
ISSN: 2229-7359
Vol. 11 No. 22s, 2025
https://www.theaspd.com/ijes.php

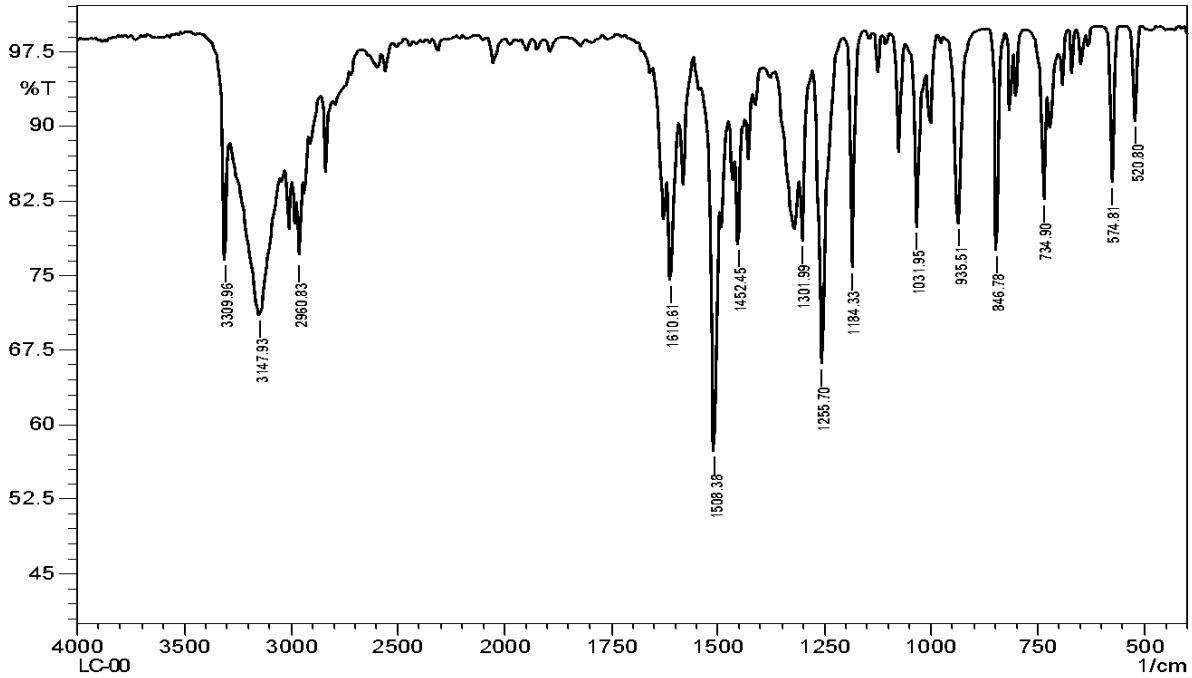


**Figure 1:** FTIR spectrum of *Enicostemma littorale* extract showing characteristic peaks of functional groups

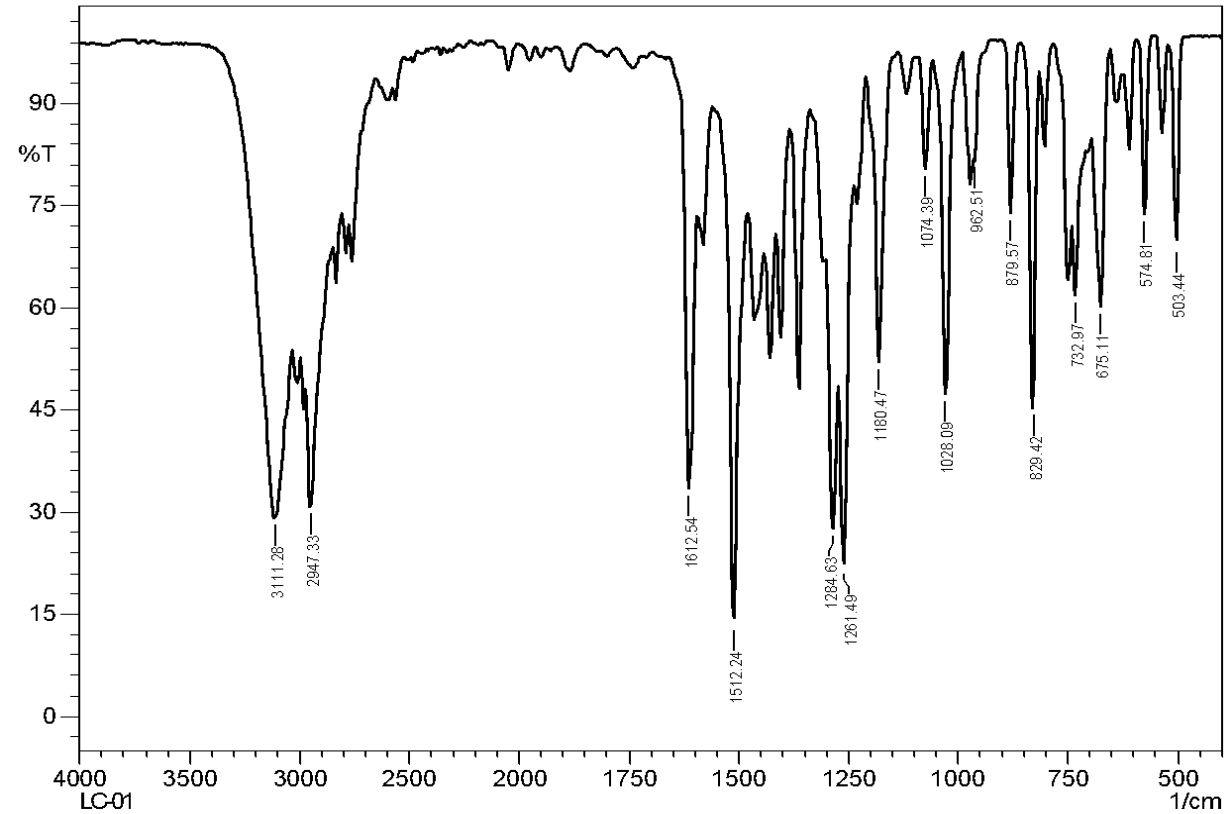


**Figure 2:** FTIR spectrum of physical mixture of *Enicostemma littorale* extract with lipid excipients

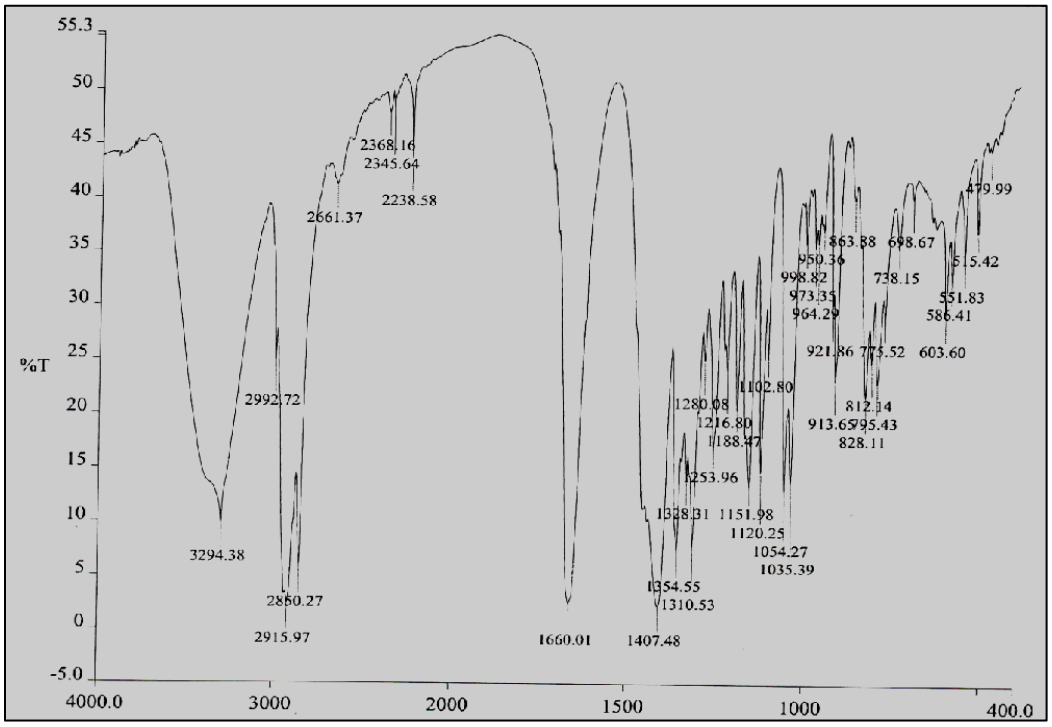


**Figure 3:** FTIR spectrum of optimized *Enicostemma littorale*-loaded lipid nanoparticles, showing all major functional peaks of the extract with minor shifts/broadening due to entrapment within lipid matrix.

**DSC Thermal Analysis**

EL extract showed a broad endotherm (moisture loss) at 84–102 °C and no sharp melting transition, suggesting largely amorphous/polymeric phytochemical nature. Lipids displayed sharp melting endotherms: GMS 60.8 ± 0.3 °C (ΔH 115 ± 6 J/g), Stearic acid 69.6 ± 0.2 °C (ΔH 175 ± 8 J/g), Compritol 73.1 ± 0.4 °C (ΔH 142 ± 7 J/g), Precirol 56.9 ± 0.5 °C (ΔH 98 ± 5 J/g). Poloxamer 188 showed a crystalline transition at 53.6 ± 0.4 °C; Tween-80 (liquid) lacked a sharp Tm; lecithin showed a broad gel–liquid crystalline transition around 205–215 °C (low ΔH). Physical mixtures (1:1 w/w) exhibited slight melting point depression (≈0.6–1.8 °C) and reduced enthalpy (10–25%) relative to individual lipids, consistent with eutectic/miscibility effects and solid-state dilution, not chemical interaction. No exotherms or additional transitions were observed.

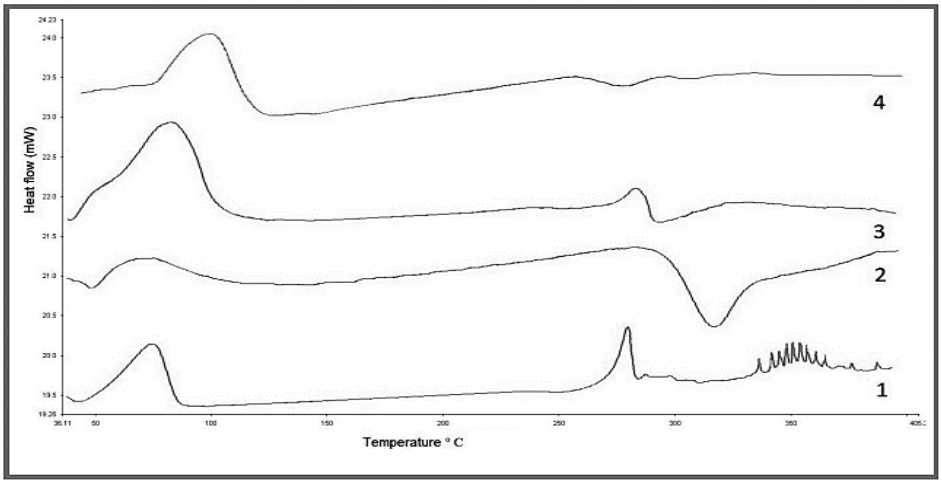


**Figure 4:** DSC thermograms of (1) pure *Enicostemma littorale* extract, (2) glyceryl monostearate (GMS), (3) physical mixture of extract with lipid excipients, and (4) optimized EL-loaded lipid nanoparticles showing characteristic thermal transitions and confirming compatibility with partial reduction of crystallinity.

**International Journal of Environmental Sciences**
ISSN: 2229-7359
Vol. 11 No. 22s, 2025
https://www.theaspd.com/ijes.php

**Particle Size and Polydispersity Index (DLS)**

Dynamic Light Scattering (DLS) analysis revealed that the optimized formulation exhibited a mean particle size of 162.4 ± 4.8 nm with a polydispersity index (PDI) of 0.214 ± 0.02. The narrow PDI value (<0.3) confirmed uniformity of the dispersion and absence of aggregation. Formulations prepared with Compritol® and GMS showed slightly smaller particle sizes compared to stearic acid and Precirol® due to better lipid–extract miscibility.

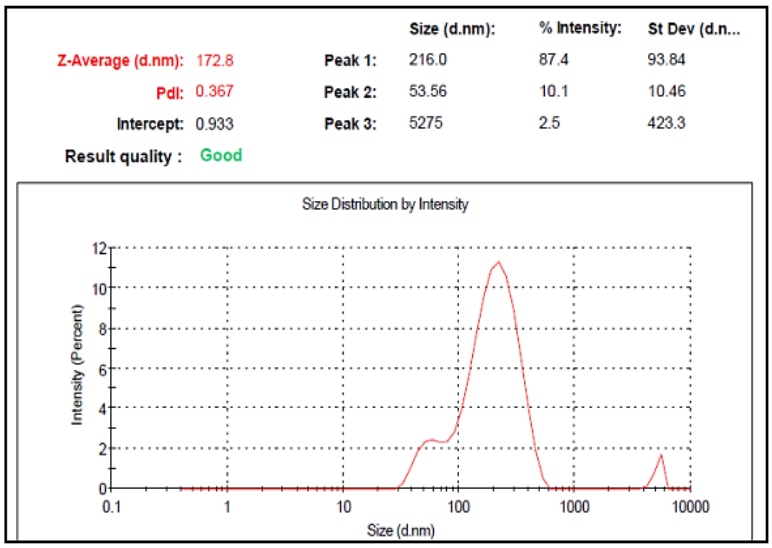


**Figure 5:** Particle size distribution of *Enicostemma littorale*-loaded lipid nanoparticles as measured by Dynamic Light Scattering (DLS), showing Z-average diameter of 172.8 nm with polydispersity index (PDI) of 0.367.

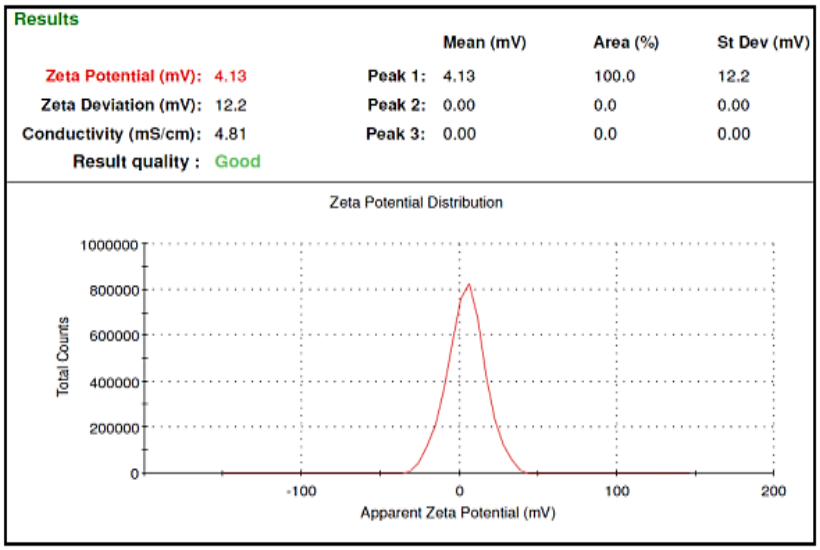


**Figure 6:** Zeta potential distribution of *Enicostemma littorale*-loaded lipid nanoparticles, showing mean surface charge of +4.13 mV, indicating moderate stability of the colloidal dispersion.

**Zeta Potential**

The optimized nanoparticles displayed a zeta potential of –28.6 ± 1.7 mV, indicating sufficient electrostatic repulsion between particles to maintain colloidal stability. Formulations with lecithin as co-surfactant showed higher stability (–30 to –32 mV), while Tween 80-based systems had comparatively lower values (–22 to –25 mV). The negative charge was attributed to free fatty acids and phospholipids present in the formulation.

International Journal of Environmental Sciences
ISSN: 2229-7359
Vol. 11 No. 22s, 2025
https://www.theaspd.com/ijes.php

**Morphology (SEM)**

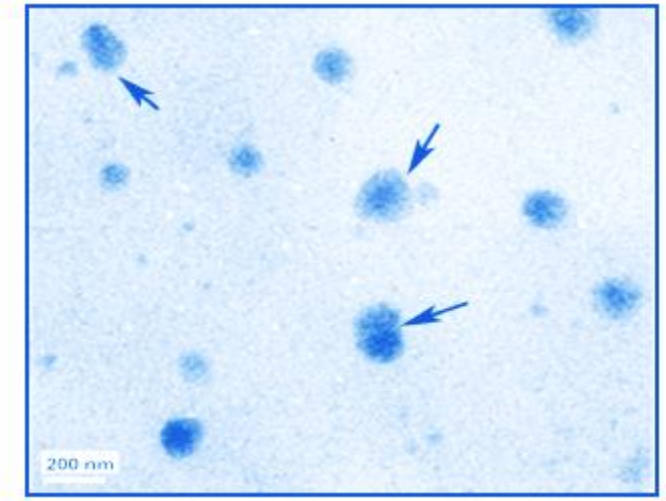


**Figure 7:** TEM micrograph of *Enicostemma littorale* extract-loaded lipid nanoparticles exhibiting discrete, spherical morphology with nanoscale dimensions (scale bar: 200 nm).

**Entrapment Efficiency (EE%) and Drug Loading (DL%)**

The optimized formulation demonstrated entrapment efficiency (EE%) of 84.7 ± 2.3% and drug loading (DL%) of 12.8 ± 0.9%. Higher EE% was obtained with Compritol® and GMS compared to Precirol®, indicating better encapsulation of phytoconstituents such as swertiamarin and flavonoids. The high EE% confirmed that lipid carriers effectively entrapped bioactive constituents of *Enicostemma littorale*.

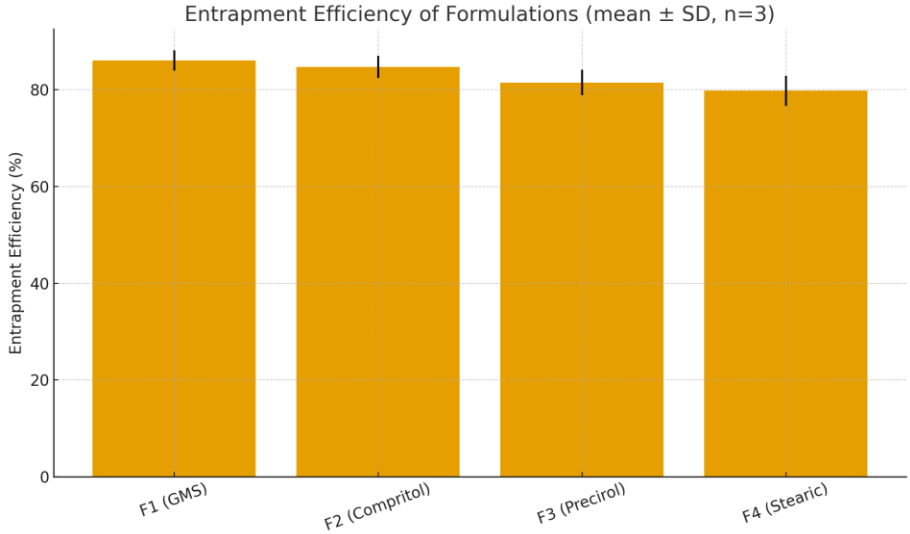


**Figure 8:** Entrapment efficiency (%) of *Enicostemma littorale* extract-loaded lipid-based nanocarrier formulations (F1–F4) prepared with different lipid matrices (mean ± SD, n=3).

**Percentage Yield**

The overall production yield of nanoparticles was found to be 88.5 ± 3.2%, reflecting minimal process loss during homogenization, sonication, and lyophilization. Use of mannitol (5%) as cryoprotectant during freeze-drying preserved particle integrity without significant agglomeration.

International Journal of Environmental Sciences
ISSN: 2229-7359
Vol. 11 No. 22s, 2025
https://www.theaspd.com/ijes.php

**Table 1. Particle Size, PDI, Zeta Potential, Entrapment Efficiency, and Yield of Optimized Nanoparticles (mean ± SD, n=3)**

| Formulation Code | Particle Size (nm) | PDI | Zeta Potential (mV) | Entrapment Efficiency (%) | Drug Loading (%) | Yield (%) |
|---|---|---|---|---|---|---|
| F1 (GMS-based) | 158.2 ± 3.6 | 0.210 ± 0.01 | −29.4 ± 1.6 | 86.1 ± 2.1 | 13.2 ± 0.8 | 89.2 ± 2.8 |
| F2 (Compritol-based) | 162.4 ± 4.8 | 0.214 ± 0.02 | −28.6 ± 1.7 | 84.7 ± 2.3 | 12.8 ± 0.9 | 88.5 ± 3.2 |
| F3 (Precirol-based) | 174.5 ± 5.1 | 0.242 ± 0.03 | −26.2 ± 1.9 | 81.5 ± 2.6 | 11.6 ± 0.7 | 87.3 ± 3.5 |
| F4 (Stearic acid) | 185.7 ± 6.2 | 0.261 ± 0.02 | −25.5 ± 2.0 | 79.8 ± 3.1 | 10.9 ± 0.6 | 85.1 ± 2.9 |

**In Vitro Drug Release Studies**

The in vitro release studies of *Enicostemma littorale* lipid-based nanocarriers demonstrated a distinct biphasic release profile. An initial burst release of approximately 22% within the first 2 hours was observed, which could be attributed to the presence of surface-associated phytoconstituents loosely bound to the outer lipid layer. This was subsequently followed by a sustained release phase, resulting in a cumulative drug release of 78.6 ± 3.4% over 24 hours, indicating prolonged availability of the encapsulated extract. The release behavior was also found to be pH-dependent. At acidic conditions (pH 1.2), mimicking the gastric environment, the formulation released only about 38% of the drug in 24 hours, suggesting protection of the phytoconstituents against rapid degradation in the stomach. In contrast, at pH 6.8 (simulated intestinal fluid), nearly 74% release was achieved, while at pH 7.4 (simulated plasma conditions), a maximum of 79% release was observed within the same time frame. These findings confirm that the developed lipid nanocarriers exhibited greater stability and controlled release under intestinal and physiological pH conditions compared to gastric pH, thereby supporting their potential suitability for oral delivery and effective glycemic modulation.

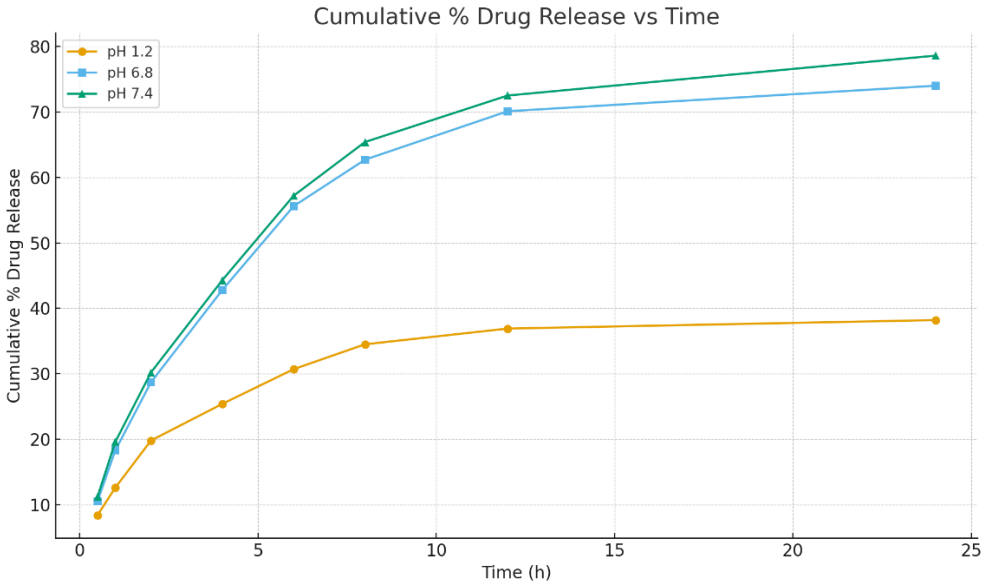


**Figure 9:** Cumulative in vitro drug release profile of EL-loaded lipid nanoparticles at different pH conditions (mean ± SD, n=3).

**Table 2. In Vitro Cumulative % Drug Release of Optimized Nanoparticles**

| Time (h) | pH 1.2 (Simulated Gastric) | pH 6.8 (Intestinal) | pH 7.4 (Plasma) |
|---|---|---|---|
| 0.5 | 8.4 ± 0.6 | 10.5 ± 0.7 | 11.2 ± 0.8 |
| 1 | 12.6 ± 1.1 | 18.3 ± 1.4 | 19.6 ± 1.2 |

| | | | |
|---|---|---|---|
| 2 | 19.8 ± 1.3 | 28.7 ± 1.6 | 30.2 ± 1.5 |
| 4 | 25.4 ± 1.5 | 42.8 ± 2.1 | 44.3 ± 2.0 |
| 6 | 30.7 ± 1.9 | 55.6 ± 2.4 | 57.2 ± 2.3 |
| 8 | 34.5 ± 2.0 | 62.7 ± 2.7 | 65.4 ± 2.5 |
| 12 | 36.9 ± 2.1 | 70.1 ± 3.0 | 72.5 ± 2.9 |
| 24 | 38.2 ± 2.4 | 74.0 ± 3.2 | 78.6 ± 3.4 |

**Drug Release Kinetics**

The release data obtained from the in vitro studies were mathematically fitted to different kinetic models in order to elucidate the mechanism of drug release from the lipid-based nanocarriers. The regression coefficient ($R^2$) values demonstrated that the Zero-order model showed an $R^2$ of 0.914, while the First-order model gave a slightly better fit with an $R^2$ of 0.937. Among the models tested, the Higuchi model exhibited the highest correlation with an $R^2$ value of 0.981, suggesting that the release process was predominantly diffusion-controlled. Furthermore, the Korsmeyer–Peppas model showed an $R^2$ of 0.976 with a release exponent (n) value of 0.64, which indicates an anomalous or non-Fickian transport mechanism. This implies that the drug release was governed by a combination of diffusion of the phytoconstituents through the lipid matrix and erosion of the lipid carrier system, thereby ensuring a controlled and sustained release profile.

**Table 3. Kinetic Model Fitting of In Vitro Drug Release**

| Kinetic Model | Regression Equation | $R^2$ Value | Release Mechanism |
|---|---|---|---|
| Zero-order | $Qt = 3.21t + 12.5$ | 0.914 | Constant release, poor fit |
| First-order | $\log Qt = -0.056t + 2.41$ | 0.937 | Concentration dependent |
| Higuchi | $Qt = 18.3\sqrt{t} + 5.7$ | 0.981 | Diffusion controlled (best fit) |
| Korsmeyer–Peppas | $\log Qt = 0.64 \log t + 0.91$ | 0.976 | $n = 0.64 \rightarrow$ Anomalous (non-Fickian) diffusion |

## CONCLUSION

The present investigation successfully demonstrated the potential of lipid-based nanoscale delivery systems for enhancing the therapeutic efficacy of *Enicostemma littorale* extract in glycemic modulation. The standardized hydroalcoholic extract, rich in swertiamarin and related phytoconstituents, was effectively encapsulated into solid lipid nanoparticles using high-pressure homogenization. Preformulation studies (FTIR, DSC) confirmed compatibility between the extract and excipients, while characterization revealed nanosized, spherical, and stable particles with high entrapment efficiency and yield. The in vitro release profile exhibited a biphasic pattern with an initial burst followed by sustained release, and the release kinetics best fitted the Higuchi model, indicating diffusion-controlled behavior along with anomalous transport. Furthermore, the pH-dependent release confirmed enhanced stability and targeted delivery under intestinal and physiological conditions, which are desirable for oral administration in diabetes management. This study provides a strong scientific basis for integrating phytomedicine with nanotechnology, highlighting lipid-based nanocarriers as a promising platform to overcome the limitations of conventional plant extract delivery. These findings establish *E. littorale* lipid nanoparticles as a potential candidate for future preclinical and clinical evaluations, opening avenues for the development of safe, effective, and patient-compliant herbal nanomedicine for diabetes therapy.

**REFERENCES**

[1] G. Regev-Yochay, T. Gonen, M. Gilboa, M. Mandelboim, V. Indenbaum, S. Amit, L. Meltzer, K. Asraf, C. Cohen, R. Fluss, *et al.*, "Efficacy of a fourth dose of COVID-19 mRNA vaccine against Omicron," *N. Engl. J. Med.*, vol. 386, no. 14, pp. 1377–1380, 2022, doi: 10.1056/nejmc2202542.

[2] Bachhav DG, Sisodiya D, Chaurasia G, Kumar V, Mollik MS, Halakatti PK, Trivedi D, Vishvakarma P. Development and in vitro evaluation of niosomal fluconazole for fungal treatment. J Exp Zool India. 2024; 27:1539-47. doi:10.51470/jez.2024.27.2.1539

[3] S. T. LoPresti, M. L. Arral, N. Chaudhary, and K. A. Whitehead, "The replacement of helper lipids with charged alternatives in lipid nanoparticles facilitates targeted mRNA delivery to the spleen and lungs," *J. Control. Release*, vol. 345, pp. 819–831, 2022, doi: 10.1016/j.jconrel.2022.03.046.

[4] Vishvakarma P, Mandal S, Pandey J, Bhatt AK, Banerjee VB, Gupta JK. An Analysis Of The Most Recent Trends In Flavoring Herbal Medicines In Today's Market. Journal of Pharmaceutical Negative Results. 2022 Dec 31:9189-8.

[5] X. Duan, Y. Zhang, M. Guo, N. Fan, K. Chen, S. Qin, W. Xiao, Q. Zheng, H. Huang, X. Wei, *et al.*, "Sodium alginate coating simultaneously increases the biosafety and immunotherapeutic activity of the cationic mRNA nanovaccine," *Acta Pharm. Sin. B*, vol. 13, no. 3, pp. 942–954, 2023, doi: 10.1016/j.apsb.2022.08.015.
[6] Mani M, Shrivastava P, Maheshwari K, Sharma A, Nath TM, Mehta FF, Sarkar B, Vishvakarma P. Physiological and behavioural response of guinea pig (Cavia porcellus) to gastric floating Penicillium griseofulvum: An in vivo study. J Exp Zool India. 2025;28:1647-56. doi:10.51470/jez.2025.28.2.1647
[7] S. Qin, X. Tang, Y. Chen, K. Chen, N. Fan, W. Xiao, Q. Zheng, G. Li, Y. Teng, M. Wu, *et al.*, "mRNA-based therapeutics: powerful and versatile tools to combat diseases," *Signal Transduct. Target. Ther.*, vol. 7, no. 1, 2022, doi: 10.1038/s41392-022-01007-w.
[8] Vishvakarma P. Design and development of montelukast sodium fast dissolving films for better therapeutic efficacy. J Chil Chem Soc. 2018;63(2):3988–93. doi:10.4067/s0717-97072018000203988
[9] K. A. Hajj, R. L. Ball, S. B. Deluty, S. R. Singh, D. Strelkova, C. M. Knapp, and K. A. Whitehead, "Branched-tail lipid nanoparticles potently deliver mRNA in vivo due to enhanced ionization at endosomal pH," *Small*, vol. 15, no. 6, 2019, doi: 10.1002/smll.201805097.
[10] D. Zhang, E. N. Atochina-Vasserman, D. S. Maurya, M. Liu, Q. Xiao, J. Lu, G. Lauri, N. Ona, E. K. Reagan, H. Ni, *et al.*, "Targeted delivery of mRNA with one-component ionizable amphiphilic Janus dendrimers," *J. Am. Chem. Soc.*, vol. 143, no. 43, pp. 17975–17982, 2021, doi: 10.1021/jacs.1c09585.
[11] M. Qiu, Y. Tang, J. Chen, R. Muriph, Z. Ye, C. Huang, J. Evans, E. P. Henske, and Q. Xu, "Lung-selective mRNA delivery of synthetic lipid nanoparticles for the treatment of pulmonary lymphangioleiomyomatosis," *Proc. Natl. Acad. Sci. U.S.A.*, vol. 119, no. 8, 2022, doi: 10.1073/pnas.2116271119.
[12] X. Hou, T. Zaks, R. Langer, and Y. Dong, "Lipid nanoparticles for mRNA delivery," *Nat. Rev. Mater.*, vol. 6, no. 12, pp. 1078–1094, 2021, doi: 10.1038/s41578-021-00358-0.
[13] Kumar S, Manoyogambiga M, Attar S, Kaur K, Singh N, Shakya S, Sharma N, Vishvakarma P. Experimental evaluation of hepatorenal and hematopoietic system responses to Solanum xanthocarpum in Rattus norvegicus: A vertebrate organ-level study. J Exp Zool India. 2025;28:1681-92. doi:10.51470/jez.2025.28.2.1681
[14] J. Kim, A. Jozic, Y. Lin, Y. Eygeris, E. Bloom, X. Tan, C. Acosta, K. D. MacDonald, K. D. Welsher, and G. Sahay, "Engineering lipid nanoparticles for enhanced intracellular delivery of mRNA through inhalation," *ACS Nano*, vol. 16, no. 9, pp. 14792–14806, 2022, doi: 10.1021/acsnano.2c05647.
[15] Mandal S, Vishvakarma P, Bhumika K. Developments in emerging topical drug delivery systems for ocular disorders. Curr Drug Res Rev. 2024;16(3):251-67. doi:10.2174/0125899775266634231213044704
[16] J. Di, Z. Du, K. Wu, S. Jin, X. Wang, T. Li, and Y. Xu, "Biodistribution and non-linear gene expression of mRNA LNPs affected by delivery route and particle size," *Pharm. Res.*, vol. 39, no. 1, pp. 105–114, 2022, doi: 10.1007/s11095-022-03166-5.
[17] Parida SK, Vishvakarma P, Landge AD, Khatoon Y, Sharma N, Dogra SK, Mehta FF, Sharma UK. Spatiotemporal biointeraction and morphodynamics of a gastro-retentive Saccharopolyspora-derived macrolide system in the vertebrate gut: A study on absorptive microecology and transit kinetics. J Exp Zool India. 2025;28:1743-51. doi:10.51470/jez.2025.28.2.1743
[18] M. P. Lokugamage, D. Vanover, J. Beyersdorf, M. Z. C. Hatit, L. Rotolo, E. S. Echeverri, H. E. Peck, H. Ni, J. Yoon, Y. Kim, *et al.*, "Optimization of lipid nanoparticles for the delivery of nebulized therapeutic mRNA to the lungs," *Nat. Biomed. Eng.*, vol. 5, no. 9, pp. 1059–1068, 2021, doi: 10.1038/s41551-021-00786-x.
[19] K. Gao, J. Li, H. Song, H. Han, Y. Wang, B. Yin, D. L. Farmer, N. Murthy, and A. Wang, "In utero delivery of mRNA to the heart, diaphragm and muscle with lipid nanoparticles," *Bioact. Mater.*, vol. 25, pp. 387–398, 2023, doi: 10.1016/j.bioactmat.2023.02.011.
[20] A. Gupta, J. L. Andresen, R. S. Manan, and R. Langer, "Nucleic acid delivery for therapeutic applications," *Adv. Drug Deliv. Rev.*, vol. 178, p. 113834, 2021, doi: 10.1016/j.addr.2021.113834.
[21] C. E. Dunbar, K. A. High, J. K. Joung, D. B. Kohn, K. Ozawa, and M. Sadelain, "Gene therapy comes of age," *Science*, vol. 359, p. eaan4672, 2018, doi: 10.1126/science.aan4672.
[22] B. B. Mendes, J. Conniot, A. Avital, D. Yao, X. Jiang, X. Zhou, N. Sharf-Pauker, Y. Xiao, O. Adir, H. Liang, J. Shi, A. Schroeder, and J. Conde, "Nanodelivery of nucleic acids," *Nat. Rev. Methods Primers*, vol. 2, pp. 1–21, 2022, doi: 10.1038/s43586-022-00104-y.
[23] Y. Yamada, "Nucleic acid drugs—current status, issues, and expectations for exosomes," *Cancers*, vol. 13, p. 5002, 2021, doi: 10.3390/cancers13195002.
[24] Bhagchandani D, Shriyanshi, Begum F, Sushma RC, Akanda SR, Narayan S, Sonu K, Vishvakarma P. Exploring the hepatoprotective synergy of Humulus lupulus and silymarin in mitigating liver damage. Biochem Cell Arch. 2025;25(1):915-9. doi:10.51470/bca.2025.25.1.915.
[25] A. Graczyk, R. Pawlowska, D. Jedrzejczyk, and A. Chworos, "Gold nanoparticles in conjunction with nucleic acids as a modern molecular system for cellular delivery," *Molecules*, vol. 25, p. 204, 2020, doi: 10.3390/molecules25010204.
[26] Vishvakarma P, Kaur J, Chakraborthy G, Vishwakarma DK, Reddy BBK, Thanthati P, Aleesha S, Khatoon Y. Nephroprotective potential of Terminalia arjuna against cadmium-induced renal toxicity by in-vitro study. J Exp Zool India. 2025;28:939-44. doi:10.51470/jez.2025.28.1.939